



HAL
open science

Preparation of Cement Clinker from Geopolymer-Based Wastes

Rabii Hattaf, Mohamed Benchikhi, Abdessamad Azzouzi, Rachida El Ouatib,
Moussa Gomina, Azzeddine Samdi, Redouane Moussa

► **To cite this version:**

Rabii Hattaf, Mohamed Benchikhi, Abdessamad Azzouzi, Rachida El Ouatib, Moussa Gomina, et al.. Preparation of Cement Clinker from Geopolymer-Based Wastes. *Materials*, 2021, 14, <10.3390/ma14216534>. <hal-03456319>

HAL Id: hal-03456319

<https://hal.science/hal-03456319v1>

Submitted on 30 Nov 2021

HAL is a multi-disciplinary open access archive for the deposit and dissemination of scientific research documents, whether they are published or not. The documents may come from teaching and research institutions in France or abroad, or from public or private research centers.

L'archive ouverte pluridisciplinaire **HAL**, est destinée au dépôt et à la diffusion de documents scientifiques de niveau recherche, publiés ou non, émanant des établissements d'enseignement et de recherche français ou étrangers, des laboratoires publics ou privés.



Distributed under a Creative Commons CC BY 4.0 - Attribution - International License

Preparation of Cement Clinker from Geopolymer-Based Wastes

Rabii Hattaf ¹, Mohamed Benchikhi ^{1,2,*}, Abdessamad Azzouzi ¹, Rachida El Ouatib ¹, Moussa Gomina ³, Azzeddine Samdi ¹ and Redouane Moussa ¹

¹ Laboratory of Physics and Chemistry of Inorganic Materials, Faculty of Sciences Ain Chock, University Hassan II Casablanca, Casablanca 53306, Morocco; rab.hattaf@gmail.com (R.H.); azzouzi.abdessamad28@gmail.com (A.A.); elouatib@yahoo.fr (R.E.O.); azdn.samdi@gmail.com (A.S.); redmoussa@yahoo.fr (R.M.)

² Department of Chemistry, Faculté Polydisciplinaire, University Sultan Moulay, Slimane, Mghila, BP.592, Beni-Mellal 23000, Morocco

³ CRISMAT UMR6508 CNRS, ENSICAEN, 6 Boulevard Maréchal Juin, CEDEX 4, 14050 Caen, France; moussa.gomina@ensicaen.fr

* Correspondence: benchikhi_mohamed@yahoo.fr

Abstract: In order to avoid potential environmental pollution from geopolymer-based material wastes, this work investigated the feasibility of using these materials as alternative raw materials in the preparation of cement clinker. The geopolymer binders and mortars were used as substitutes for natural mineral clays since they are rich in silica and alumina. Simulated geopolymer wastes were prepared by the activation of metakaolin or fly ash by an alkaline silicate solution. The cement-clinkers fired at 1450 °C for 1h were characterized by XRD, XRF, SEM-EDS, and a free lime (CaO_f) content test. The anhydrous clinker mineral phases C₃S (Ca₃SiO₅), C₂S (Ca₂SiO₄), C₃A (Ca₃Al₂O₆), and C₄AF (Ca₄Al₂Fe₂O₁₀) were well-crystallized in all investigated formulations. The free lime was lower than 1.3 wt% in all elaborated clinkers, which indicates a high degree of clinkerization. The results demonstrate that geopolymer binder and mortar materials are suitable substitutes for natural mineral clay incement clinker preparation.

Keywords: geopolymer; waste; clinker; alternative raw materials



Citation: Hattaf, R.; Benchikhi, M.; Azzouzi, A.; El Ouatib, R.; Gomina, M.; Samdi, A.; Moussa, R. Preparation of Cement Clinker from Geopolymer-Based Wastes. *Materials* **2021**, *14*, 6534. <https://doi.org/10.3390/ma14216534>

Academic Editor: Eddie Koenders

Received: 8 September 2021

Accepted: 28 September 2021

Published: 30 October 2021

Publisher's Note: MDPI stays neutral with regard to jurisdictional claims in published maps and institutional affiliations.



Copyright: © 2021 by the authors. Licensee MDPI, Basel, Switzerland. This article is an open access article distributed under the terms and conditions of the Creative Commons Attribution (CC BY) license (<https://creativecommons.org/licenses/by/4.0/>).

1. Introduction

Geopolymers are a class of alkaline aluminosilicate materials, synthesized by the activation of various reactive aluminosilicate materials of geological origin (e.g., metakaolin) or industrial by-products (e.g., fly ash) by a concentrated alkali hydroxide silicate solution. These materials have several advantages: easy preparation, low curing temperature (i.e., ≤100 °C), reduced gas emissions, and good properties [1,2]. For these reasons, geopolymer materials are considered a promising and sustainable ecological alternative to conventional materials, especially cement and ceramics.

In recent years, geopolymer materials have been adopted in many fields, including construction and civil engineering (as binders, mortars, concretes, light weight panels and bricks for thermal and acoustic insulation, protective coating, low-cost ceramics, and fire protection structures) [2–7]. These fields are considered among the highest producers of solid waste in the world. Therefore, it is essential to propose anticipatory strategies in parallel for the good management and elimination of this type of waste. These strategies must accompany the progressive introduction of these materials into the construction materials market, and consequently avoid their accumulation in huge quantities or their disposal in landfills. In addition, environmental concerns have become a global priority in recent decades, pushing towards sustainable practices for the recovery of waste and by-products. Furthermore, the valorization of geopolymer-based material wastes can contribute to the conservation of finite, natural, non-renewable resources. In this

context, a very limited number of initiatives have focused on the recycling of geopolymer waste. These studies generally remain within the framework of a single approach, which consists in reusing the waste in the form of aggregates to replace natural aggregates (sand or gravel) in order to produce mortars or concretes. Hattaf et al. [8] proposed to reuse geopolymer waste as a substitute for the starting raw materials (metakaolin and fly ash) to produce new geopolymer matrices. These authors demonstrated that high compressive strengths can be maintained for substitution rates up to 40 wt% (compressive strengths greater than 43 MPa). A. Akbarnezhad and S. Mesgari [9] studied the substitution of natural aggregates by recycled geopolymer concrete wastes in the form of coarse aggregates for the production of geopolymer or Portland cement concretes. Their results showed that the total substitution of natural aggregates resulted in only 12.9, 10.7, and 15.2% decreases in compressive strength, modulus of elasticity, and modulus of rupture, respectively. P. Zhu et al. [10] studied the replacement of river sand aggregates by recycled geopolymer aggregates for the preparation of metakaolin-based mortars. They showed that the mechanical strength of the prepared mortars is unchanged up to a substitution rate of about 50 wt%. A. Gharzouni et al. [11] developed metakaolin-based geopolymer matrices by substituting metakaolin with relatively fine aggregates of recycled geopolymers. The results showed that the feasibility of these materials is limited to a substitution rate of about 20%.

Geopolymer binders and mortars are very rich in silica and alumina. Thus, these materials have considerable potential as substitutes for natural mineral clay in the preparation of cement clinkers. To the best of our knowledge, the valorization of geopolymer materials in clinker production has not yet been reported. Therefore, this work aims to prove the feasibility of using geopolymer binders and mortar powders as cement raw materials. The cementclinkers were prepared by partially replacing natural mineral clay with geopolymer binders or mortar powders. The simulated geopolymer materials were obtained through the activation of metakaolin or fly ash by an alkaline silicate solution. The prepared materials were characterized mainly by X-ray diffraction (XRD), scanning electron microscopy coupled with energy-dispersive X-ray spectroscopy (SEM-EDS), and X-ray fluorescence (XRF).

2. Materials and Methods

2.1. Materials, Equipment, and Methods

The metakaolin (MK) used in this work was supplied by Imerys company reference Agrical M1000 (Paris, France). The fly ash (FA) was obtained from the JarFlasfar thermal power station (El Jadida, Morocco). The silica fume (SF) used in this work was exploited by a local cement manufacturing company. The standard sand used to prepare the mortars was provided by Nouvelle du Littoral Company (Leucate, France). The sodium silicate solution (45 wt%) with molar ratio $\text{SiO}_2/\text{Na}_2\text{O} = 2$ was supplied by Cadilhac Society. Sodium hydroxide NaOH (98%), calcium carbonate CaCO_3 (99%), and iron oxide Fe_2O_3 (99%) used in this work were of analytical grade.

The chemical composition of powders was determined via wavelength dispersive X-ray fluorescence analysis (WDXRF). The WDXRF measurements were performed using a Thermo ARL 9800XP spectrometer (ThermoFisher[®], Waltham, MA, USA) equipped with an X-ray tube, with a maximum power of 3.0 kW. (30 kV and 80 mA). It was calibrated using certified reference material standards (CRMs) from the same matrix as the samples to be analyzed. A calibration curve was established for each element, and the correlation coefficients were determined by regression calculation. The content of the elements was evaluated by using the ADVANTX-2252 instrument operating with v2.6.3.3985D of the OXSAS software (ThermoFisher[®], Waltham, MA, USA). The samples were prepared by forming them into fused glass discs. To prepare the glass disc samples, 4 g of the dried sample was mixed with 4 g of dilithium tetraborate (spectroflux 100) and was then melted in a furnace at 1000 °C for 1h. After that, the homogeneous melted sample was recast into glass beads that were 2 mm thick and 32 mm in diameter. The loss on ignition (LOI) was

measured at 1000 °C. The chemical composition of metakaolin, fly ash, limestone, silica fume, and sand was determined by using X-ray fluorescence; this is summarized in Table 1. The metakaolin and fly ash are mainly composed of silica and alumina. It should be noted that the fly ash contains an appreciable amount of Fe_2O_3 , CaO, and MgO. Sand and silica fume powders are mainly composed of SiO_2 . The limestone powder contains more than 56% of CaO, with an ignition loss of 43%.

Table 1. Chemical composition of metakaolin, fly ash, limestone, silica fume, and sand.

Raw Materials	Oxides (wt%)									
	SiO_2	Al_2O_3	Fe_2O_3	CaO	MgO	SO_3	Na_2O	K_2O	P_2O_5	LOI
Metakaolin	57.38	37.11	1.41	0.43	0.36	0.19	0.18	0.81	0.06	2.08
Fly Ash	51.48	22.57	5.86	4.79	2.21	0.51	0.62	1.10	0.86	10.01
Limestone	0.21	0.08	0.02	56.13	0.26	0.20	0.01	0.01	0.01	43.08
Silica Fume	93.86	0.27	0.04	0.96	1.28	0.20	0.18	0.30	0.09	2.82
Sand	97.81	0.45	0.06	0.39	0.08	0.22	0.10	0.24	0.02	0.63

The nature of the crystalline phase present in the powders was investigated by using X-ray diffraction measurements. XRD patterns were obtained at room temperature using a Bruker D8 (Bruker, Madison, WI, USA), employing $\text{CuK}\alpha$ radiation as the X-ray source (operating voltage was 40 kV and current was 40 mA). XRD data were collected in the 10–70° 2θ range, with a 0.059° step-scan and at 5 s per step. The XRD patterns of metakaolin (MK), fly ash (FA), limestone (LM), and silica fume (SF) are given in Figure 1. All XRD peaks of limestone can be attributed to calcite (JCPDS: 88-1807). XRD reveals the amorphous nature of the silica fume. The XRD pattern of metakaolin shows a mixture of quartz (JCPDS: 46-1045) and residual kaolinite (JCPDS: 29-1488) in addition to the main amorphous phase. The fly ash powder is largely amorphous, with a small amount of mullite (JCPDS: 15-0776) and quartz phases. These results are in perfect agreement with the XRF analysis.

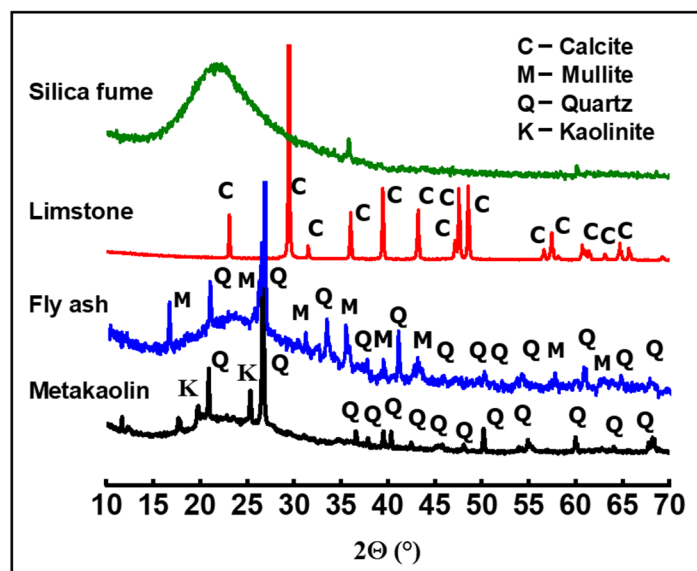


Figure 1. XRD patterns of metakaolin, fly ash, limestone, and silica fume powders.

The thermal behavior of powders was studied using a DTG 60 instrument from Shimadzu (Shimadzu, Kyoto, Japan). Analyses were performed in air using a heating rate of 10 °C/min. The DTA-TG curves of metakaolin and fly ash is presented in Figure 2. The thermal decomposition of fly ash occurred in two steps (Figure 2a): In the first step, the mass loss in the TG curve below 100 °C can be attributed to the departure of adsorbed water. This phenomenon is associated with endothermic effects at 20–75 °C in the DTA

curve. In the second step, a mass loss of about 8% is observed in the temperature range of 600–800 °C in the TG graph, accompanied by an exothermic peak in the DTA curve. This weight loss could be attributed to the decomposition of calcite (CaCO_3) present in the sample [12]. The TG curve of metakaolin (Figure 2b) indicates that there are several mass losses up to 650 °C. These could be attributed to the evaporation of adsorbed water and the dehydroxylation of residual kaolinite ($\text{Al}_2\text{Si}_2\text{O}_5(\text{OH})_4$). The weak exothermic peak observed at around 994 °C in the DTA curve can be related to the crystallization of mullite [13,14]. The particle size distribution was investigated with a Laser analyzer Mastersizer 2000 instrument (Malvern Instruments, Worcestershire, UK). Figure 3 shows the particle size distribution curves of all raw materials. These curves show a d_{50} of 6.67, 8.44, 4.27, and 9.31 μm for metakaolin, fly ash, limestone, and silica fume, respectively.

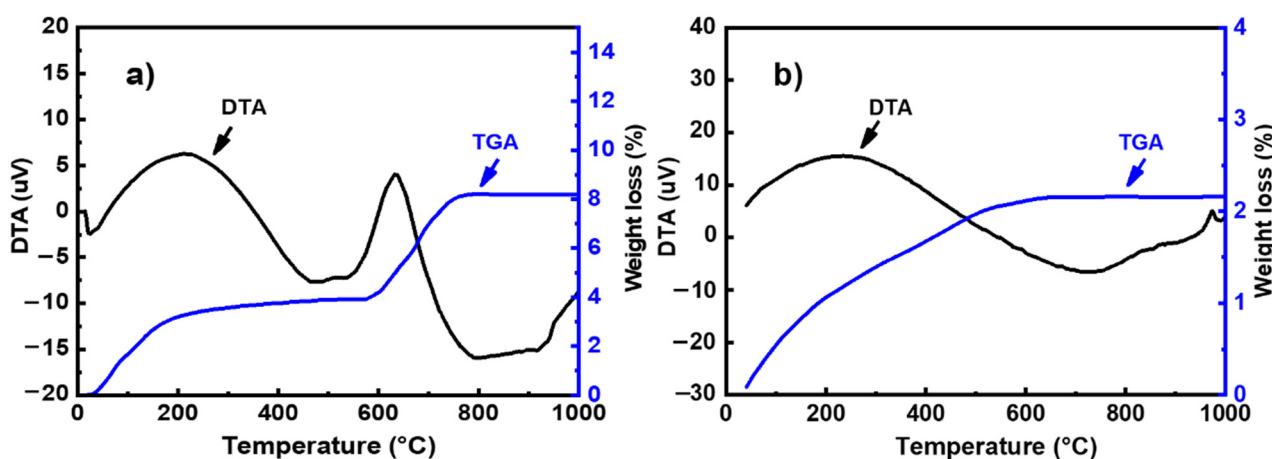


Figure 2. TG–DTA curves for (a) metakaolin and (b) fly ash.

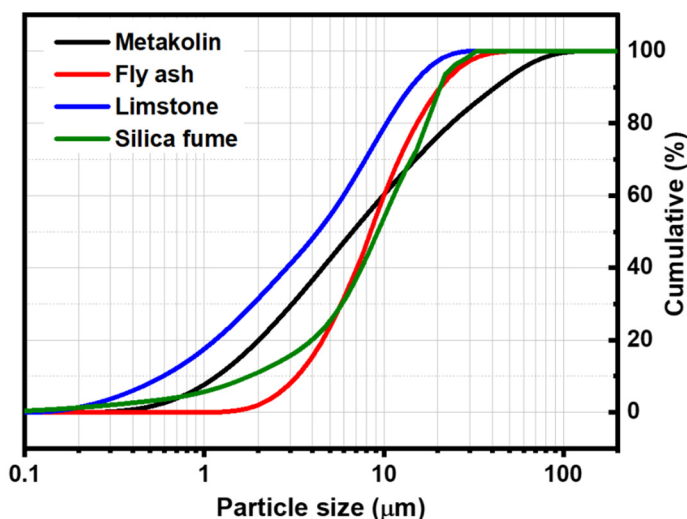


Figure 3. Particle size distribution of input material powders.

2.2. Preparation of Geopolymer-Based Materials

The preparation of geopolymer materials was carried out in accordance with our previous study [8]. The procedure for geopolymer preparation is shown in Figure 4. The geopolymer materials were obtained through the reaction between an activator solution and the metakaolin or fly ash powders. Initially, the activator solution (AS), with a weight ratio of $\text{SiO}_2/\text{Na}_2\text{O} = 1.2$, was prepared by mixing sodium silicate, sodium hydroxide, and water. The obtained solution was stirred for 24 h at room temperature before use. Then, the activator solution was mixed with the metakaolin or fly ash powders. After that, the mixture was mechanically mixed until the homogenization of the geopolymer pastes. The weight

ratio of the liquid (AS)/aluminosilicate source (metakaolin or fly ash) was 0.83 and 0.58 for the metakaolin-based geopolymer binder (BGMK) and the fly ash-based geopolymer binder (BGFA), respectively. To prepare geopolymer mortars, standard sand was added to the geopolymer paste at the weight ratio of sand:aluminosilicate source = 70:30. The obtained materials were named MGMK and MGFA for metakaolin and fly ash-based mortars, respectively. The geopolymer binders and mortars were cast into polypropylene molds and vibrated to remove air bubbles. Then, the molds were sealed with a polyethylene film to prevent the rapid evaporation of water. The specimens were then cured at 60 °C/5 h and 80 °C/20 h for metakaolin-based materials (BGMK and MGMK) and fly ash-based materials (BGFA and MGFA), respectively. The geopolymer materials were stored for a year in open air in order to simulate aging in an ambient environment and were subsequently crushed using a roller mill. The geopolymer materials were ground into fine powders to be able to use them as raw materials that would replace clay in the production of cement clinkers by the conventional sintering process.

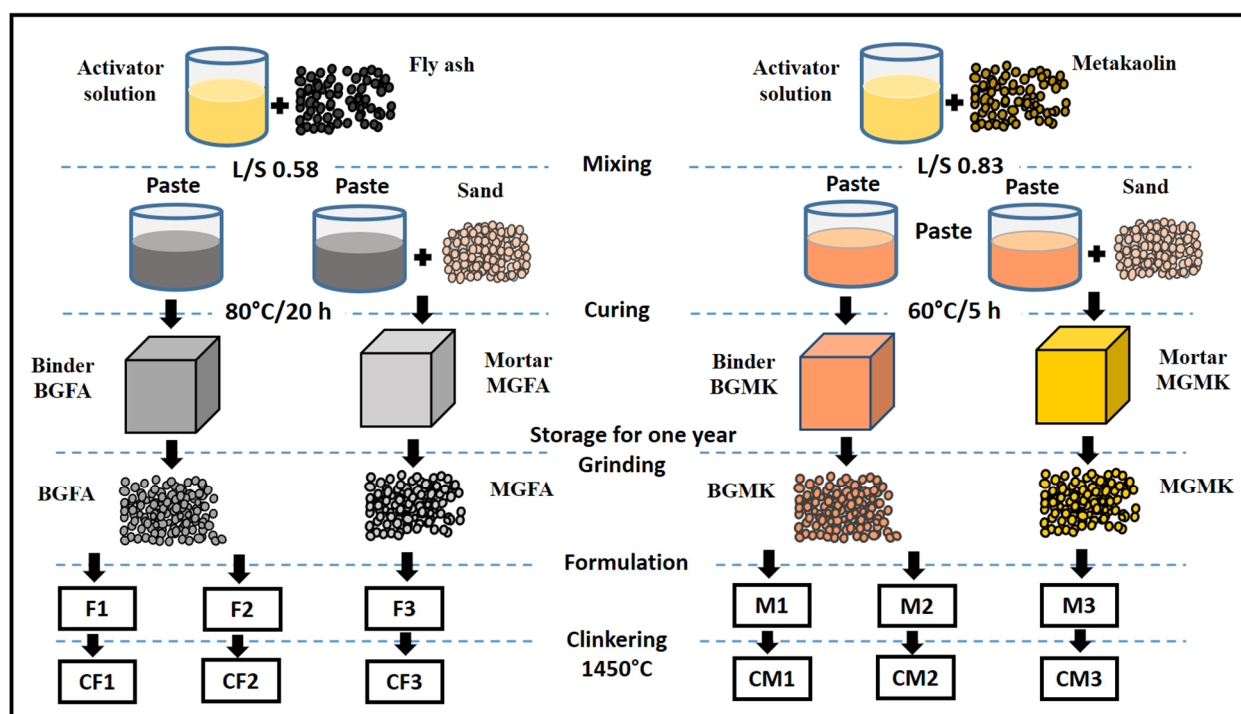


Figure 4. Flowchart representing the procedure for the preparation of cement clinker from geopolymer-based materials.

2.3. Clinker Preparation

It is well-known that the chemical composition of a geopolymer binder/mortar is very different from that of a cement clinker [15]. Therefore, geopolymer powders are mixed with calcium carbonate and corrective materials to adjust the clinker formulation. The preparation of cement clinker is controlled by the lime saturation factor (LSF), silica ratio (SR), and alumina ratio (AR), which are calculated according to Equations (1)–(3):

$$\text{LSF} = (C / (2.8S + 1.2A + 0.6F)) \quad (1)$$

$$\text{SR} = (S / (A + F)) \quad (2)$$

$$\text{AR} = (A / F) \quad (3)$$

where C, S, A, F are CaO, SiO₂, Al₂O₃, and Fe₂O₃, respectively.

The values of LSF, SR, and AR were set at 92–98, 2–3.7, and 1.0–4.0, respectively (ASTM C 150-97). As shown in Table 2, six formulations were investigated in this study. The ingredients of formulations were calculated according to the chemical composition of

raw materials (Tables 1 and 3). To investigate the reactivity of geopolymer amorphous phases, we designed formulations F1 and M1 by replacing a high proportion of mineral clay (>67 wt%) with geopolymer BGMK and BGFA binders. The formulations F2, M2, F3, and M3 were designed to produce clinker with low Na₂O content. The reaction mixtures were ground to ensure good homogeneity. Then, they were poured into a platinum crucible and heated in a muffle furnace under air at a temperature rate of 5 °C/min. The firing cycle involved three steps: (i) heating at 1000 °C for 1 h in order to promote the complete decomposition of carbonates, (ii) heating at 1450 °C for 1 h to promote the complete crystallization of the calcium-silicate and calcium-iron-aluminate phases, (iii) air quenching to prevent the crystallization of the γ -C₂S phase.

Table 2. Investigated formulations (wt%).

Raw Materials	Formulations (wt%)					
	M1	F1	M2	F2	M3	F3
Limestone	76.86	74.01	78.35	76.83	78.63	76.93
Metakaolin	-	-	6.76	-	6.50	-
Fly Ash	-	-	-	12.17	-	12.19
BGMK	15.53	-	3.74	-	-	-
BGFA	-	21.08	-	2.75	-	-
MGMK	-	-	-	-	13.20	-
MGFA	-	-	-	-	-	10.04
Silica fume	5.82	4.30	9.49	7.41	-	-
Fe ₂ O ₃	1.79	0.60	1.66	0.85	1.67	0.85

Table 3. Chemical composition of geopolymer-based materials.

Raw Materials	Oxides (wt%)									
	SiO ₂	Al ₂ O ₃	Fe ₂ O ₃	CaO	MgO	SO ₃	Na ₂ O	K ₂ O	P ₂ O ₅	LOI
BGFA	47.05	17.34	5.49	5.45	2.12	0.55	6.64	1.66	0.58	13.11
BGMK	54.42	25.35	1.09	1.21	0.28	0.31	8.06	0.68	0.10	8.49
MGFA	84.02	5.04	1.53	1.77	0.64	0.31	1.88	0.63	0.17	4.02
MGMK	84.79	7.92	0.37	0.64	0.14	0.25	2.49	0.37	0.04	2.99

3. Results and Discussion

3.1. Geopolymer-Based Raw Materials

As mentioned above, one of the main objectives of this work was to demonstrate the reactivity and the conversion of geopolymer amorphous phases into clinker phases. Simulated geopolymer-based material wastes were prepared using two aluminosilicate sources: metakaolin and fly ash. The aluminosilicate source was activated by an alkaline silicate solution. This solution provided sufficient alkalinity to dissolve the amorphous aluminosilicate powders while inhibiting the formation of a gel at an early stage, thus covering the aluminosilicate particles, which hindered further dissolution. Moreover, the activating solution provided the soluble silicate species necessary for the polycondensation reaction to obtain a compact connected network with a high degree of geopolymerization [16–19]. The XRD patterns of geopolymer binders are given in Figure 5. The XRD pattern of the metakaolin-based geopolymer shows peaks characteristic of quartz and residual kaolin. These crystalline phases were initially present in the metakaolin precursor as impurities and resisted in the activation process. However, the XRD pattern of fly ash-based geopolymer shows a mixture of quartz and mullite phases. These refractory phases resisted the activation process. Both patterns show a broad halo peak at a low 2-theta position (between 20° and 40°), which indicates the presence of amorphous phases. These results agree well with those recently reported in the literature [18,19]. It is well-known that the geopolymer phases are amorphous in nature. In our case, all the observed XRD peaks

can be attributed to the unreacted crystal precursors. The amorphous phases observed in our materials represent mainly the formation of sodium aluminosilicate gel. The samples were also investigated with a scanning electron microscope (Tescan VEGA 3) (Tescan Orsay Holding, Brno-Kohoutovice, Czech Republic) provided with energy-dispersive X-ray spectroscopy (EDS) (Oxford Instruments, Oxford, UK). As seen in the SEM micrographs (Figure 6), the two geopolymer binders are composed mainly of amorphous phases, indicating a high degree of geopolymerization [20,21]. Close inspection of the SEM images revealed the presence of the unreacted precursor particles in the fly ash-based geopolymer (Figure 6b) [21,22].

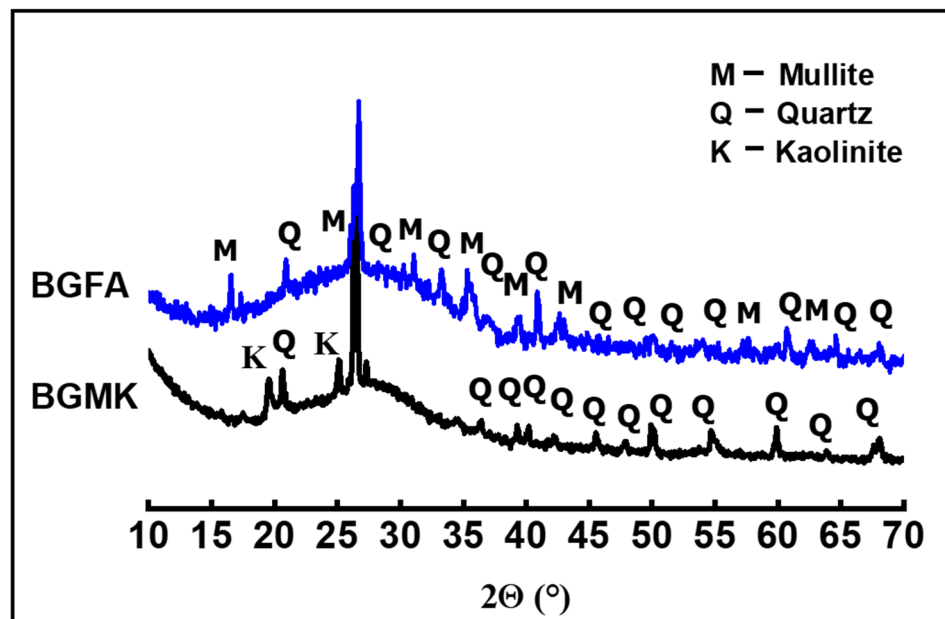


Figure 5. XRD patterns of BGMK and BGFA geopolymer binders.

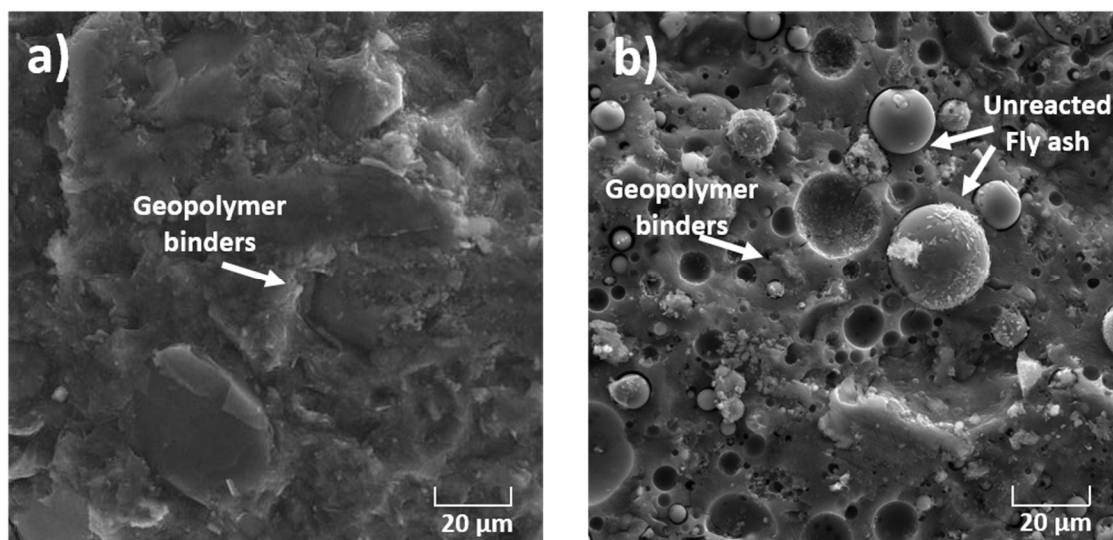


Figure 6. SEM micrographs of (a) BGMK and (b) BGFA geopolymer binders.

The thermal behavior of geopolymer binders was investigated by thermal analysis (Figure 7). As seen in Figure 7a, the TG curve of the BGMK binder shows a successive mass loss of about 8% below 200 °C. These weight losses are accompanied by two endothermic peaks at 75 °C and 125 °C in the DTA curve. According to Rodríguez et al. [23], these mass

losses originated in the free water trapped in the pores and zeolitic water available in the reaction products, which can easily be removed from the alkaline silicate gel surface at this temperature. However, the TGA curve of the fly ash-based geopolymer (Figure 7b) shows weight loss in two steps. The weight loss observed below 200 °C, associated with an endothermic peak at 75 °C in the DTA curve, can be attributed to the departure of adsorbed water from the sample [24]. A second mass loss of about 4% is observed in the temperature range of 450–650 °C, accompanied by exothermic effects in the DTA curve. This weight loss could be assigned to the decomposition of calcium hydroxide (Ca(OH)₂) [21,25].

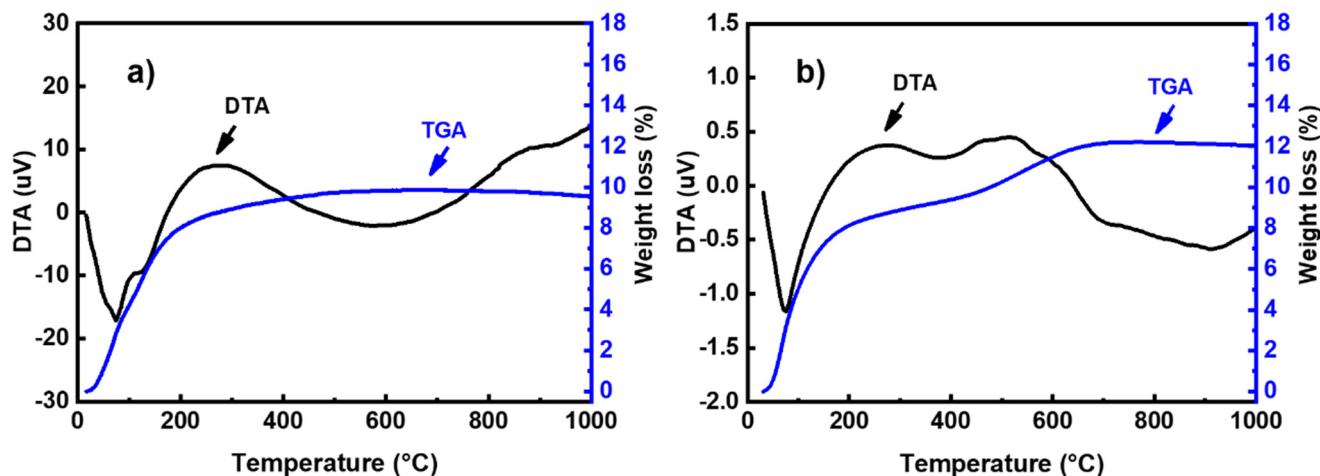


Figure 7. TGA/DTA curves of (a) BGMK and (b) BGFA geopolymer binders.

The chemical composition of geopolymer binders and geopolymer mortars are given in Table 3. The geopolymer binders are mainly composed of SiO₂ and Al₂O₃. The relatively high content of Na₂O (>6%) in both geopolymer binders comes from the activator solution. The chemical composition of the geopolymer mortars MGFA and MGMK are similar, with minor differences in their oxide content. Their SiO₂ content is higher than 80%, which is due to the presence of standard sand. However, the Al₂O₃ content of the geopolymer mortars is relatively low compared to geopolymer binders. The geopolymer-based materials are composed mainly of SiO₂ and Al₂O₃, which are suitable substitutes of mineral clays in the preparation of cement clinker [26]. Moreover, these materials contain low amounts of CaO, Fe₂O₃, and MgO. In order to use the geopolymer-based materials as raw materials instead of clay in the preparation of cement clinker, they were first crushed to reduce their initial size. Then, they were loaded into the ball mill for the final grinding. It has been demonstrated by many research groups that particle size plays a crucial role in the solid-state reaction [27]. Figure 8 shows the particle size distribution of the different geopolymer-based powders. As can be seen, all geopolymer-based materials were reduced to powders composed of fine particles (d₅₀ between 7 and 10 μm).

3.2. Cement Clinkers

Several steps have been proposed to explain the formation of cement clinker [28]:

- (i) Formation of intermediate reactive oxides by dehydration/dehydroxylation and decomposition of clay at temperatures lower than 950 °C;
- (ii) Formation of metal oxides (i.e., CaO, MgO) by carbonate decomposition at 550–1000 °C;
- (iii) Crystallization of the calcium aluminate CA (CaO·Al₂O₃) and ferroaluminate C2AF (2CaO·Al₂O₃·Fe₂O₃). Then, conversion of CaO, CS, CA, and Fe₂O₃ into the ferrite C4AF, tricalcium aluminate C3A, and belite C2S phases. These reactions occur in the temperature range of 550–1280 °C, according to the following Equations:





- (iv) Formation of the alite phase C_3S by the chemical reaction of free CaO with C_2S ; melting of C_4AF at temperatures higher than 1280°C . The molten C_4AF medium promotes the growth of the pre-existing C_2S and C_3S phases in the reaction mixture at this temperature range.

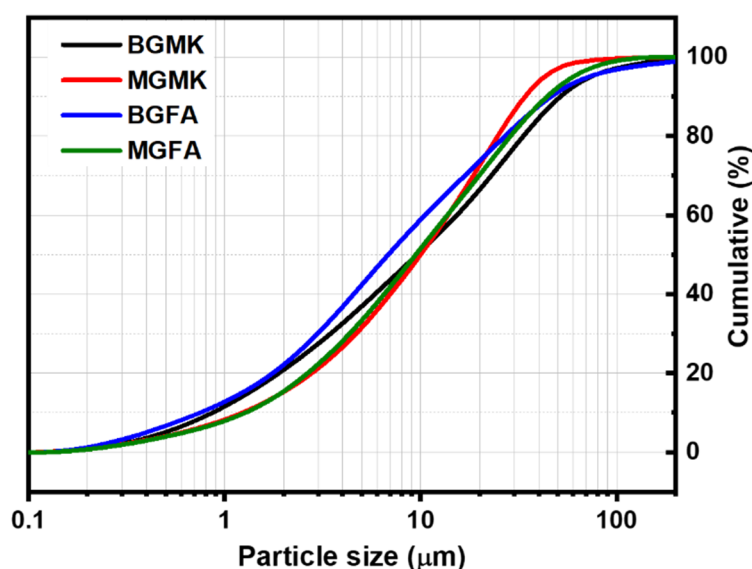


Figure 8. Particle size distribution curves for the ball-milled geopolimer wastes.

The chemical composition of the investigated clinkers are given in Table 4. As can be seen, the chemical composition of all clinkers is very similar, except the Na_2O content. The high alkali content observed in the CM1 and CF1 clinkers was caused by the high amount of geopolimer binders incorporated into the reaction mixture (Table 2). As discussed previously, the Na_2O content of geopolimer binders is greater than 6 wt% (Table 3). The alkali content of cement clinkers is a crucial parameter that influences the properties of concrete. Indeed, the high alkali content of the clinker induces the reaction of $\text{Na}_2\text{O}/\text{K}_2\text{O}$ with aggregates in concrete, thus causing the expansion and cracking of the materials [29]. The alkali equivalent content $\text{Na}_2\text{O}_{\text{eq}}$ was calculated according to Equation (7) [30].

$$\text{Na}_2\text{O}_{\text{eq}} = \text{Na}_2\text{O} + 0.658 \text{K}_2\text{O} \quad (7)$$

Table 4. Chemical composition of the produced cement clinkers.

Portland Cement Clinker	Oxides (wt%)									
	SiO_2	Al_2O_3	Fe_2O_3	CaO	MgO	SO_3	Na_2O	K_2O	P_2O_5	LOI
CM1	21.42	6.10	2.97	65.95	0.49	0.32	1.88	0.19	0.04	0.64
CF1	21.48	5.66	2.64	65.25	1.06	0.42	2.15	0.57	0.20	0.57
CM2	22.76	5.38	2.72	66.98	0.55	0.30	0.48	0.16	0.03	0.63
CF2	22.41	5.19	2.66	67.00	0.95	0.37	0.38	0.30	0.20	0.52
CM3	22.86	5.32	2.74	67.13	0.38	0.31	0.48	0.16	0.02	0.62
CF3	22.70	5.04	2.58	67.05	0.81	0.38	0.38	0.30	0.19	0.58

As seen in Table 5, the alkali equivalent content ($\text{Na}_2\text{O}_{\text{eq}}$) values of the formulations CM1 and CF1 are larger than the maximum acceptable value defined by the Standard ASTM C 150-97 [30]. However, when the natural clay mineral was replaced with an adequate proportion of geopolimer-based material (clinkers CM2, CF2, CM3, and CF3), the alkali equivalent content ($\text{Na}_2\text{O}_{\text{eq}}$) was less than 0.6 wt%.

Table 5. Mineralogical composition of the prepared cement clinkers.

Mineralogical Phases (%)	Portland Cement Clinker						ASTM C 150-97
	CM1	CF1	CM2	CF2	CM3	CF3	
C ₃ S	55.79	55.47	54.75	58.75	54.8	57.70	50–70
C ₂ S	19.65	20.05	24.27	20.25	24.5	21.88	15–35
C ₃ A	11.15	10.53	9.66	9.24	9.46	8.99	5–12
C ₄ AF	9.02	8.04	8.27	8.09	8.32	7.84	5–15
Quality Indexes							
SR (%)	2.36	2.59	2.81	2.86	2.84	2.98	2.0–3.7
AR (%)	2.06	2.14	1.98	1.95	1.94	1.95	1.0–4.0
LSF (%)	94	93	92	93	92	92	92–98
Na ₂ O _{eq} (wt %)	2.01	2.52	0.59	0.58	0.59	0.58	0.6
CaO _f (wt %)	1.12	1.23	1.18	1.23	1.25	1.26	0.5–1.5

The mineralogical composition of the investigated clinkers determined according to Bogue equations (Equations (8)–(11)) is shown in Table 5. The C₃S, C₂S, C₃A, C₄AF phase contents of all clinkers are very similar and conform to the standard specification for Portland cement clinker. Furthermore, the lime saturation factor (LSF), silica ratio (SR), and alumina ratio (AR) of all cement clinkers are in the recommended ranges for Portland cement (Table 5). These results indicate the ideal amount of lime, silica, alumina, and iron oxide in our formulations. Free lime (f-CaO) content detected by the glycerol-ethanol method is less than 1.3 wt% for all clinkers, which indicates a relatively high degree of clinkerization [31–33].

$$C_3S (\%) = 4.071(CaO) - 7.602(SiO_2) - 6.718(Al_2O_3) - 1.43(Fe_2O_3) \quad (8)$$

$$C_2S (\%) = 2.87(SiO_2) - 0.754(C_3S) \quad (9)$$

$$C_3A (\%) = 2.65(Al_2O_3) - 1.692(Fe_2O_3) \quad (10)$$

$$C_4AF (\%) = 3.043(Fe_2O_3) \quad (11)$$

The XRD patterns of the prepared clinkers are presented in Figure 9. In the patterns of all clinkers fired at 1450 °C, mixtures of four phases were identified: alite C₃S (JCPDS: 49-0442), belite C₂S (JCPDS: 33-0302), tricalcium aluminate C₃A (JCPDS: 38-1429), and ferrite C₄AF (JCPDS: 30-0226). The characteristic XRD peaks of lime were not observed in any pattern, which indicates a very low CaO_f content in our clinkers. Likewise, the γ-C₂S phase was not crystallized in any of our samples, which is probably due to the quenching treatment [34]. The high degree of crystallization of clinker phases and the low amount of free lime suggests a high degree of clinkerization.

Furthermore, the microstructure of the prepared clinkers was investigated by SEM-EDS analysis. The SEM image of clinker CF3 along with the energy spectra is represented in Figure 10 as a typical example. The C₃S crystal is seen to have a different form and a size less than 40 μm. Small C₂S grains are also observed in the SEM image. Finally, the interstitial phase observed in the SEM image is composed of Ca, Si, Al, and Fe, which can be attributed to C₄AF and C₃A melting together and interweaving with each other.

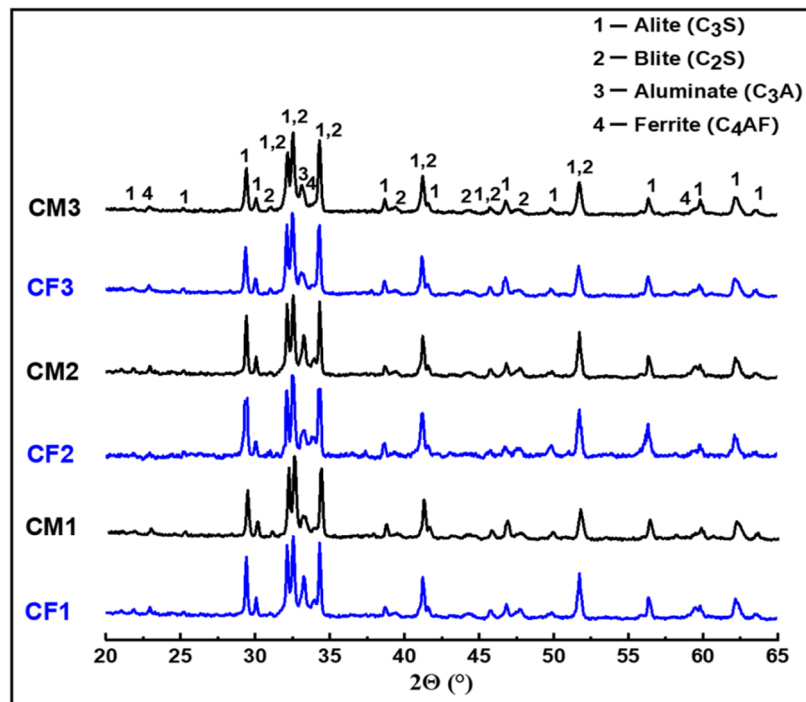


Figure 9. XRD patterns of the prepared clinkers.

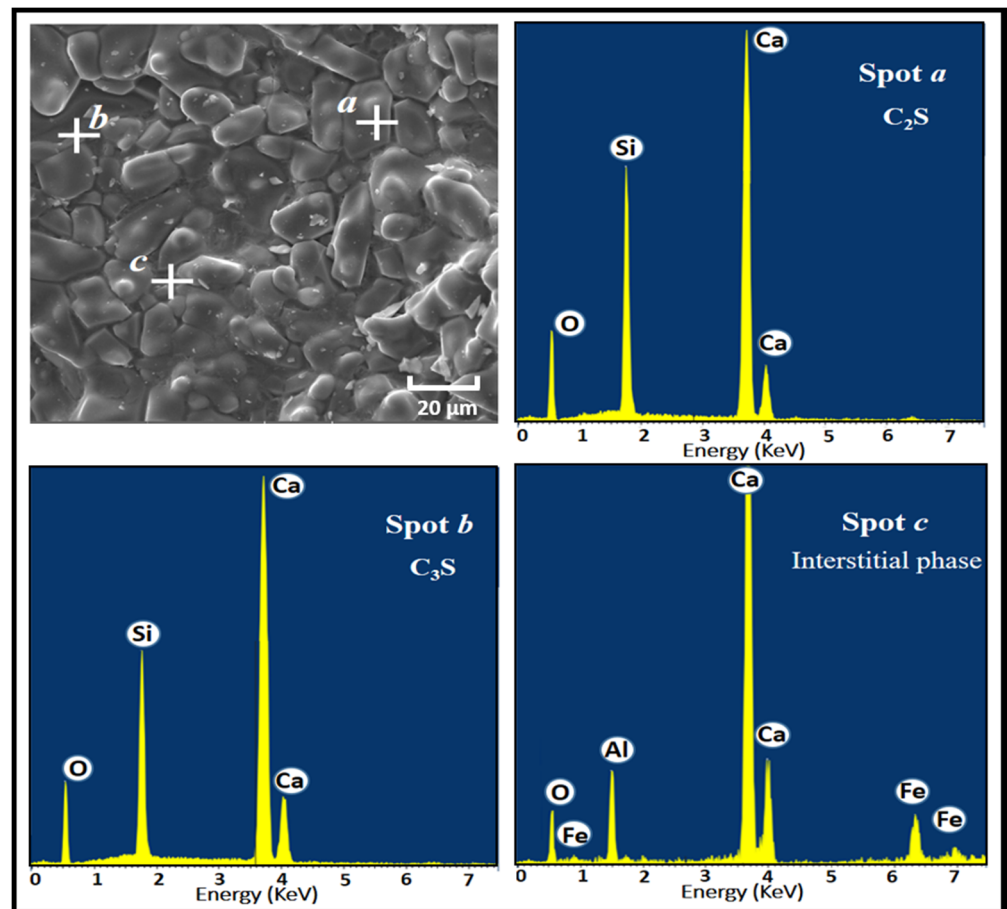


Figure 10. SEM micrograph and EDS spectra of the cement clinker CF3.

4. Conclusions

In this study, cement clinkers were prepared using geopolymer-based materials as raw materials. Four different geopolymer-based materials were investigated: the metakaolin-based geopolymer binder (BGMK) and mortar (MGMK), and the fly ash-based geopolymer binder (BGFA) and mortar (MGFA). The chemical analysis carried out by XRF revealed that these materials are very rich in silica and alumina, which can be suitable substitutes of mineral clays in the preparation of clinker. In all investigated formulations, the crystalline phases identified by XRD after clinkerization at 1450 °C were C₃S, C₂S, C₄A, C₄AF. The free lime content was less than 1.3 wt% in all samples, indicating a high degree of clinkerization. Chemical analysis revealed that the amount of geopolymer wastes incorporated into the clinker mixture was limited by the equivalent alkali (Na₂O_{eq}) content. The Na₂O_{eq} content was kept at less than 0.6 wt% when the natural clay was substituted with 17.3 wt%, 11.8 wt%, 61.8 wt%, and 43.50 wt% of BGMK, BGFA, MGMK, and MGFA, respectively. We expect these results to provide a theoretical basis for the recovery of geopolymer wastes in the production of cement clinker.

Author Contributions: Conceptualization, R.H.; methodology, R.E.O. and A.S.; validation, M.B., R.M. and M.G.; formal analysis, R.E.O. and A.A.; investigation, R.H. and M.B.; resources, R.M. and A.S.; data curation, R.H. and A.A.; writing—original draft preparation, R.H. and M.B.; writing—review and editing, M.B. and R.M.; visualization, R.H. and A.A.; supervision, R.M.; funding acquisition, R.M. and M.G. All authors have read and agreed to the published version of the manuscript.

Funding: This research is supported through the R&D Initiative—Appel à projets autour des phosphates APPHOS—sponsored by OCP, OCP Foundation, R&D OCP, Mohammed VI Polytechnic University, National Center of Scientific and Technical Research CNRST, Ministry of Higher Education, Scientific Research and Professional Training of Morocco MESRSFC under the project ID * MAT-MOS-01/2017 *.

Institutional Review Board Statement: Not applicable.

Informed Consent Statement: Not applicable.

Conflicts of Interest: The authors declare no conflict of interest.

References

1. Davidovits, J. Properties of Geopolymer Cements. In Proceedings of the 1st International Conference on Alkaline Cements and Concretes, Scientific Research Institute On Binders and Materials, Kiev, Ukraine, 1994; pp. 131–149. Available online: <http://www.geopolymer.org/wp-content/uploads/KIEV.pdf> (accessed on 28 September 2021).
2. Provis, J.L.; Van Deventer, J.S.J. *Geopolymers: Structures, Processing, Properties and Industrial Applications*; Elsevier: Amsterdam, The Netherlands, 2009; ISBN 9781845694494.
3. Fazli, H.; Yan, D.; Zhang, Y.; Zeng, Q. Effect of Size of Coarse Aggregate on Mechanical Properties of Metakaolin-Based Geopolymer Concrete and Ordinary Concrete. *Materials* **2021**, *14*, 3316. [[CrossRef](#)]
4. Jiang, C.; Wang, A.; Bao, X.; Ni, T.; Ling, J. A review on geopolymer in potential coating application: Materials, preparation and basic properties. *J. Build. Eng.* **2020**, *32*, 101734. [[CrossRef](#)]
5. Ngouloure, Z.N.M.; Nait-Ali, B.; Zekeng, S.; Kamseu, E.; Melo, U.C.; Smith, D.; Leonelli, C. Recycled natural wastes in metakaolin based porous geopolymers for insulating applications. *J. Build. Eng.* **2015**, *3*, 58–69. [[CrossRef](#)]
6. Prochon, P.; Zhao, Z.; Courard, L.; Piotrowski, T.; Michel, F.; Garbacz, A. Influence of Activators on Mechanical Properties of Modified Fly Ash Based Geopolymer Mortars. *Materials* **2020**, *13*, 1033. [[CrossRef](#)]
7. Singh, N.B. Fly Ash-Based Geopolymer Binder: A Future Construction Material. *Minerals* **2018**, *8*, 299. [[CrossRef](#)]
8. Hattaf, R.; Aboulayt, A.; Samdi, A.; Lahlou, N.; Ouazzani Touhami, M.; Gomina, M.; Moussa, R. Reusing Geopolymer Waste from Matrices Based on Metakaolin or Fly Ash for the Manufacture of New Binder Geopolymeric Matrices. *Sustainability* **2021**, *13*, 8070. [[CrossRef](#)]
9. Akbarnezhad, A.; Huan, M.; Mesgari, S.; Castel, A. Recycling of geopolymer concrete. *Constr. Build. Mater.* **2015**, *101*, 152–158. [[CrossRef](#)]
10. Zhu, P.; Hua, M.; Liu, H.; Wang, X.; Chen, C. Interfacial evaluation of geopolymer mortar prepared with recycled geopolymer fine aggregates. *Constr. Build. Mater.* **2020**, *259*, 119849. [[CrossRef](#)]
11. Gharzouni, A.; Vidal, L.; Essaidi, N.; Joussein, E.; Rossignol, S. Recycling of geopolymer waste: Influence on geopolymer formation and mechanical properties. *Mater. Des.* **2016**, *94*, 221–229. [[CrossRef](#)]

12. Buruberry, L.H.; Seabra, M.P.; Labrincha, J.A. Preparation of clinker from paper pulp industry wastes. *J. Hazard. Mater.* **2015**, *286*, 252–260. [[CrossRef](#)] [[PubMed](#)]
13. Samet, B.; Mnif, T.; Chaabouni, M. Use of a kaolinitic clay as a pozzolanic material for cements: Formulation of blended cement. *Cem. Concr. Compos.* **2007**, *29*, 741–749. [[CrossRef](#)]
14. Wan, Q.; Rao, F.; Song, S. Reexamining calcination of kaolinite for the synthesis of metakaolin geopolymers—Roles of dehydroxylation and recrystallization. *J. Non. Cryst. Solids* **2017**, *460*, 74–80. [[CrossRef](#)]
15. Xu, G.; Zhong, J.; Shi, X. Influence of graphene oxide in a chemically activated fly ash. *Fuel* **2018**, *226*, 644–657. [[CrossRef](#)]
16. Cai, J.; Li, X.; Tan, J.; Vandevyvere, B. Thermal and compressive behaviors of fly ash and metakaolin-based geopolymer. *J. Build. Eng.* **2020**, *30*, 101307. [[CrossRef](#)]
17. Gao, K.; Lin, K.L.; Wang, D.; Hwang, C.L.; Shiu, H.S.; Chang, Y.M.; Cheng, T.W. Effects SiO₂/Na₂O molar ratio on mechanical properties and the microstructure of nano-SiO₂ metakaolin-based geopolymers. *Constr. Build. Mater.* **2014**, *53*, 503–510. [[CrossRef](#)]
18. Cho, Y.K.; Yoo, S.W.; Jung, S.H.; Lee, K.M.; Kwon, S.J. Effect of Na₂O content, SiO₂/Na₂O molar ratio, and curing conditions on the compressive strength of FA-based geopolymer. *Constr. Build. Mater.* **2017**, *145*, 253–260. [[CrossRef](#)]
19. Yuan, J.; He, P.; Jia, D.; Yang, C.; Zhang, Y.; Yan, S.; Yang, Z.; Duan, X.; Wang, S.; Zhou, Y. Effect of curing temperature and SiO₂/K₂O molar ratio on the performance of metakaolin-based geopolymers. *Ceram. Int.* **2016**, *42*, 16184–16190. [[CrossRef](#)]
20. Zidi, Z.; Ltifi, M.; Zafar, I. Synthesis and attributes of nano-SiO₂ local metakaolin based-geopolymer. *J. Build. Eng.* **2021**, *33*, 101586. [[CrossRef](#)]
21. Jiang, X.; Zhang, Y.; Xiao, R.; Polaczyk, P.; Zhang, M.; Hu, W.; Bai, Y.; Huang, B. A comparative study on geopolymers synthesized by different classes of fly ash after exposure to elevated temperatures. *J. Clean. Prod.* **2020**, *270*, 122500. [[CrossRef](#)]
22. Durak, U.; İlkentapar, S.; Karahan, O.; Uzal, B.; Atiş, C.D. A new parameter influencing the reaction kinetics and properties of fly ash based geopolymers: A pre-rest period before heat curing. *J. Build. Eng.* **2020**, *35*, 102023. [[CrossRef](#)]
23. Rodríguez, E.D.; Bernal, S.A.; Provis, J.L.; Paya, J.; Monzo, J.M.; Borrachero, M.V. Effect of nanosilica-based activators on the performance of an alkali-activated fly ash binder. *Cem. Concr. Compos.* **2013**, *35*, 1–11. [[CrossRef](#)]
24. Hosan, A.; Haque, S.; Shaikh, F. Compressive behaviour of sodium and potassium activators synthesized fly ash geopolymer at elevated temperatures: A comparative study. *J. Build. Eng.* **2016**, *8*, 123–130. [[CrossRef](#)]
25. Chindapasirt, P.; Rattanasak, U.; Taebuanhuad, S. Resistance to acid and sulfate solutions of microwave-assisted high calcium fly ash geopolymer. *Mater. Struct. Constr.* **2013**, *46*, 375–381. [[CrossRef](#)]
26. Nettleship, I.; Slavick, K.G.; Kim, Y.J.; Kriven, W.M. Phase Transformations in Dicalcium Silicate: I, Fabrication and Phase Stability of Fine-Grained β Phase. *J. Am. Ceram. Soc.* **1992**, *75*, 2400–2406. [[CrossRef](#)]
27. González-Velasco, J.R.; Ferret, R.; López-Fonseca, R.; Gutiérrez-Ortiz, M.A. Influence of particle size distribution of precursor oxides on the synthesis of cordierite by solid-state reaction. *Powder Technol.* **2005**, *153*, 34–42. [[CrossRef](#)]
28. Chatterjee, A.K. Chemico-Mineralogical characteristics of raw materials. In *Advances in Cement Technology*; Pergamon Press: Oxford, UK, 1983; pp. 39–68.
29. Shi, Z.; Leemann, A.; Rentsch, D.; Lothenbach, B. Synthesis of alkali-silica reaction product structurally identical to that formed in field concrete. *Mater. Des.* **2020**, *190*, 108562. [[CrossRef](#)]
30. ASTM C 150-97—Standard Specification for Portland Cement; ASTM International: West Conshohocken, PA, USA, 1997.
31. Papamarkou, S.; Christopoulos, D.; Tsakiridis, P.E.; Bartzas, G.; Tsakalakis, K. Vitrified medical wastes bottom ash in cement clinkerization. Microstructural, hydration and leaching characteristics. *Sci. Total. Environ.* **2018**, *635*, 705–715. [[CrossRef](#)]
32. Young, G.; Yang, M. Preparation and characterization of Portland cement clinker from iron ore tailings. *Constr. Build. Mater.* **2019**, *197*, 152–156. [[CrossRef](#)]
33. Liu, X.; Jin, J.; Wu, W.; Herz, F. A novel support vector machine ensemble model for estimation of free lime content in cement clinkers. *ISA Trans.* **2020**, *99*, 479–487. [[CrossRef](#)]
34. Cuesta, A.; Losilla, E.R.; Aranda, M.A.G.; Sanz, J.; De La Torre, Á.G. Reactive belite stabilization mechanisms by boron-bearing dopants. *Cem. Concr. Res.* **2012**, *42*, 598–606. [[CrossRef](#)]